Spectral properties of (854) Frostia, (1333) Cevenola and (3623) Chaplin

Mirel Birlan, Dan Alin Nedelcu, Pascal Descamps, Jerôme Berthier, Franck Marchis, Sihane Merouane, Marcel Popescu

Monthly Notices
of the
ROYAL ASTRONOMICAL SOCIETY

Mon. Not. R. Astron. Soc. **415,** 587–595 (2011) doi:10.1111/j.1365-2966.2011.18740.x

Spectral properties of (854) Frostia, (1333) Cevenola and (3623) Chaplin

M. Birlan,[1⋆] D. A. Nedelcu,[2] P. Descamps,[1] J. Berthier,[1] F. Marchis,[3] S. Merouane[4] and M. Popescu[1]

[1]*Institut de Mécanique Céleste et de Calcul des Éphémérides (IMCCE), Observatoire de Paris, 77 avenue Denfert-Rochereau, 75014 Paris Cedex, France*
[2]*Astronomical Institute of the Romanian Academy, 5 Cuţitul de Argint, RO-040557 Bucharest, Romania*
[3]*University of California at Berkeley, Department of Astronomy, 601 Campbell Hall, Berkeley, CA 94720, USA*
[4]*University Paris VII, Department of Physics, 75206 Paris Cedex, France*

Accepted 2011 March 17. Received 2011 March 15; in original form 2010 September 10

ABSTRACT

Near-infrared spectroscopy can play a key role in establishing the mineralogical composition of objects and supporting other physical data obtained by complementary observational techniques such as adaptive optics, radar and photometry. The objective of our survey was asteroids that present large variations in their light curves. We report observations for asteroids (854) Frostia, (1333) Cevenola and (3623) Chaplin carried out in the 0.8–2.5 μm spectral range using SpeX/Infrared Telescope Facility (IRTF) in LowRes mode. The spectral modelling of these asteroids gives new insights into these peculiar objects in the main belt. (854) Frostia is a V-type asteroid, and its spectral properties are similar to those of basalts. The most probable mineralogical solution $Wo_8Fs_{43}En_{49}$ was calculated for Frostia. (1333) Cevenola was estimated to have an S_q spectral type, in agreement with its membership of the Eunomia family. (3623) Chaplin is an S-type asteroid, in agreement with the taxonomic type of the Koronis family.

Key words: techniques: spectroscopic – minor planets, asteroids: individual: (854) Frostia – minor planets, asteroids: individual: (1333) Cevenola – minor planets, asteroids: individual: (3623) Chaplin.

1 INTRODUCTION

The light curve of an asteroid is a display of the variation of its magnitude over time. The light curve is related to the rotation of an asteroid around an instantaneous axis. In other words, the light curve could be interpreted as an observable of the angular momentum for a given object. The resulting variation is primarily due to the shape (French & Binzel 1989). The light curve could be also due to albedo variation (Harris & Lupishko 1989) of asteroids. The results of observations of light curves for asteroids are regularly synthesized in catalogues of light curves (for example Lagerkvist et al. 1987).

Several asteroids exhibit large-amplitude light curves, which remained unexplained until the last decade. Several explanations were proposed for these variations, starting with elongated shaped asteroids and including double and multiple systems of aggregates in a weak self-gravitational field (Cellino et al. 1985).

The number of known multiple systems among asteroids has increased significantly in recent years. In the past, the binarity and multiplicity of asteroids was suggested by several authors (van Flandern, Tedesco & Binzel 1979) based on occultations of stars (for example in the articles of Binzel (1978)[1] and Donnison (1979)[2]) or photoelectric photometry (Dunlap & Gehrels 1969; Binzel & van Flandern 1979; Tedesco 1979). These observational facts were the origin of theoretical problems related to spin evolution and stability (Wijesinghe & Tedesco 1979; Zappala et al. 1980; Leone et al. 1984).

Several articles are based on observations using various techniques, namely radar (Ostro et al. 2000, 2002; Magri et al. 2007), adaptive optics (Marchis et al. 2005), adaptive optics combined with light-curve photometry (Descamps et al. 2007) and light-curve photometry (Pravec et al. 2002; Behrend et al. 2006).

Analytical and numerical simulations of catastrophic collisions among small bodies, using several hypotheses, have been published regularly by several teams (Durda et al. 2004; Dell'Oro & Cellino 2007; Holsapple & Michel 2008). This topic remains open, despite the important acquisition of knowledge from laboratory experiments and numerical tests. In the framework of this paper, the most important conclusion of these works is that elongated shapes, binarity or multiplicity could be explained for both large objects

[1] The article also presents historical facts of the occultation of stars by asteroids.
[2] This satellite was not confirmed by direct imaging (Storrs et al. 1999).

⋆E-mail: Mirel.Birlan@imcce.fr

(≈100 km in size) and relatively small ones (kilometre-size asteroids). For instance, a *doublet system* is a binary system in which both bodies are of nearly equal size. Their origin is not well understood, but several such systems have been reported (e.g. (90) Antiope, (617) Patroclus, (69230) Hermes, 1998WW31). Theoretical studies concerning the movement of components around their centre of mass can be validated with observational results (obtained for instance using adaptive optics); results for their dynamics will be constrained by the physical model, which takes into account the shape, bulk density and internal properties of the components. Furthermore, the interaction between a dynamical and a physical model allows the derivation of the most probable configuration of the system (in terms of separation of components, orbital parameters, shapes and densities).

Spectroscopic measurements of asteroids contribute to the characterization of minerals at the surface. In the assumption of homogeneous bodies, this constrains the nature of tensile stress inside the object. The features of an object's spectrum constrain the mineralogical composition and implicitly the range of its density. By applying these considerations to the models, some physical parameters such as macroporosity or *rubble-pile* structures will be derived.

The article is focused on the spectroscopy of one binary system and two asteroids with large-amplitude light curves. Near-infrared (NIR) spectroscopic observations for the binary system of (854) Frostia are presented. Observations of (1333) Cevenola and (3623) Chaplin, asteroids with large-amplitude light curves, are also presented. A detailed analysis of these spectra is carried out and the models derived for each asteroid are then discussed.

2 THE OBSERVING PROTOCOL

The asteroids were observed in the 0.8–2.5 μm spectral region by means of the instrument SpeX on the Infrared Telescope Facility (IRTF) located on Mauna Kea, Hawaii. These observations were performed in remote mode from the Centre d'Observation à Distance en Astronomie à Meudon (CODAM), more than 12 000 km away from Hawaii, (Birlan et al. 2004, 2006) using the low-resolution prism mode ($R = 100$) of the spectrograph. We used a 0.8×15 arcsec^2 slit oriented north–south. The spectra for the asteroid and the solar analogue stars were obtained alternately on two separate locations on the slit denoted A and B (the *nodding* procedure). The data-reduction process consists of two main steps: (1) obtaining the raw spectra for the object and the solar analogue and (2) computation of the normalized reflectance spectrum by dividing the asteroid spectrum by the solar analogue spectrum and performing a correction for telluric lines.

For the first step, the Image Reduction and Analysis Facility (IRAF; http://iraf.noao.edu) was used. For the second step, after the wavelength calibration, specific IDL routines were also used in order to diminish the influence of telluric bands in our spectra (Rivkin et al. 2004). In order to publish high-confidence data, the raw images were also re-reduced via SPEXTOOL (Cushing, Vacca & Rayner 2004) and specific MIDAS procedures, and the results were compared with the previous ones.

Our strategy was to observe all asteroids as close to the zenith as possible (the circumstances of our targets are presented in Table 1). Thus, we managed to observe all targets with an airmass lower then 1.25. No other correction for the differential refraction was considered. Each observed asteroid was preceded by observations of solar analogues in the vicinity (airmass differences between the asteroid and the standard of less (than 0.1). The seeing varied between 0.7–1.8 arcsec during the observing runs, and the humidity was in the 25–85 per cent range.

In order to obtain a signal-to-noise ratio (S/N) in the 80–200 range, we needed 15–40 min of exposure time, depending on the asteroid magnitude, and counting both the effective exposure and CCD camera readout time. The circumstances of the observations are presented in Table 2.

For the asteroid spectra, the solar analogues HD 127913, G104−335 and HD 73708 were observed. For the computation of the final reflectance (ratio between the asteroid spectrum and the star spectrum) we took into account the similar dynamic regimes of the detector (Vacca, Cushing & Rayner 2004; Rayner et al. 2003).

Table 1. Circumstances of the observations are presented (date of observations with the fraction of day for the beginning of the observation, number and name of the asteroid, semimajor axis, eccentricity, inclination, apparent magnitude, phase angle and heliocentric and geocentric distances).

Date (UT)	Asteroid	a (UA)	e	i (°)	V	Φ (°)	r (UA)	Δ (UA)
2007/03/13.48753	(854) Frostia	2.36823	0.17398	6.090	14.93	3.62	2.34843	1.36087
2007/03/12.54861	(1333) Cevenola	2.63584	0.13314	14.642	15.63	13.74	2.66963	1.82769
2007/03/13.57463	(1333) Cevenola	2.63584	0.13314	14.642	15.61	13.45	2.67108	1.82177
2007/03/12.37775	(3623) Chaplin	2.85048	0.08790	3.072	17.15	14.68	3.03656	2.30870
2007/03/13.26730	(3623) Chaplin	2.85048	0.08790	3.072	17.17	14.89	3.03710	2.31966

Table 2. Observation circumstances for each asteroid. The columns show the name of the asteroid, the mean Julian Date (JD) value for each series, the individual time for each spectrum (I time), the number of cycles and the airmass at the mean JD of each series. The final two columns present the standard star used for data reduction and its airmass during the observation.

Object	JD	Itime (s)	Cycles	Airmass	Standard	Airmass
(854) Frostia	2454172.98754	120	10	1.105	G104−335	1.070
(1333) Cevenola	2454172.04901	120	24	1.016	HD 127913	1.055
(1333) Cevenola	2454173.07464	120	10	1.034	HD 127913	1.031
(3623) Chaplin	2454171.87776	120	18	1.111	HD 73708	1.085
(3623) Chaplin	2454172.76731	120	20	1.019	HD 73708	1.018

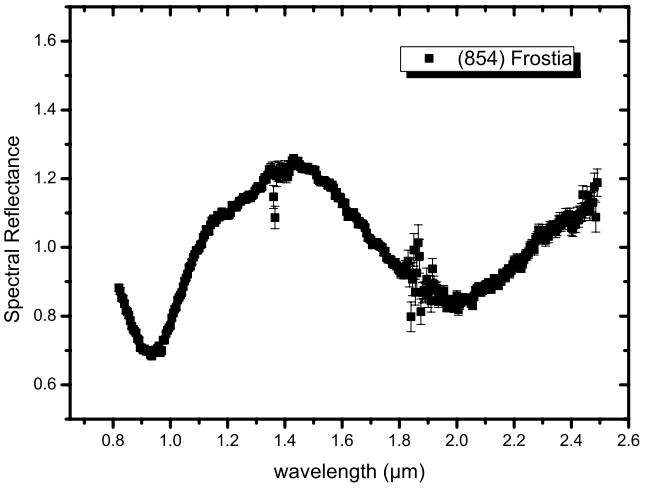

Figure 1. NIR spectrum of (854) Frostia with error bars. The spectrum is normalized to 1.25 μm.

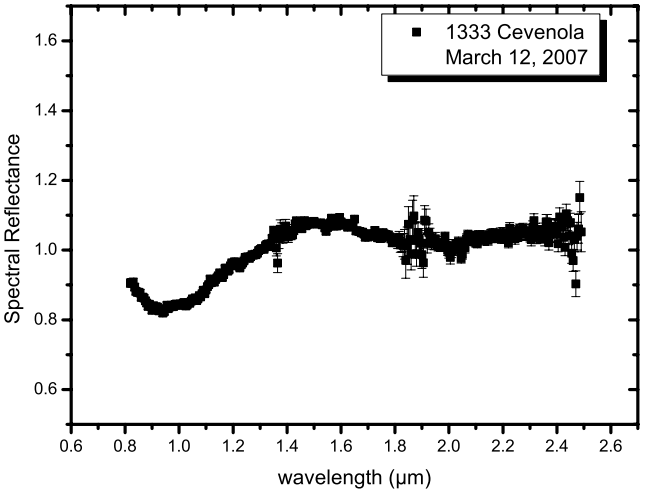

Figure 2. NIR spectrum of (1333) Cevenola obtained on 2007 March 12 with error bars. The spectrum is normalized to 1.25 μm.

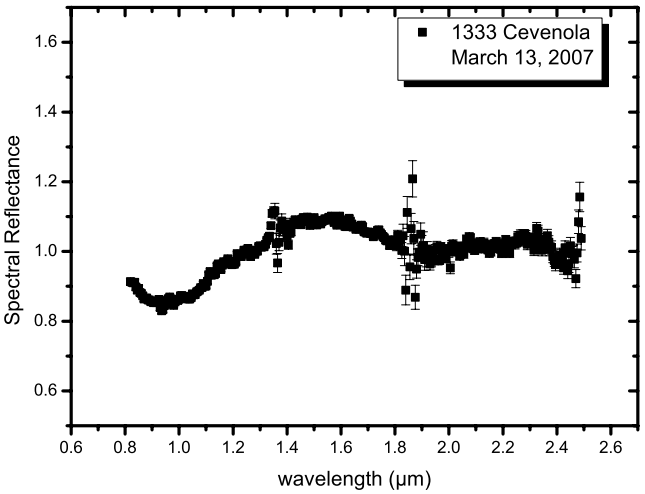

Figure 3. NIR spectrum of (1333) Cevenola obtained on 2007 March 13 with error bars. The spectrum is normalized to 1.25 μm.

3 RESULTS

3.1 (854) Frostia

This asteroid was observed intensely in photometry (Behrend et al. 2006) by amateurs and professional astronomers.[3] The asteroid is a slow rotator with a synodic period of 37.728 h. Its regular light curve with an amplitude of 0.33 mag presents, for short periods of time, important attenuation of about 0.7–0.8 mag. The large magnitude is very well explained by mutual eclipse/occultation events for an object with two components of comparable size. Based on a physical model of a double system, Behrend et al. (2006) calculated a bulk density of 750–1020 kg m^{-3}. They explain such a low density value by a possible C-type asteroid with a high macroporosity of about 45 per cent.

Sloan Digital Sky Survey (SDSS) colours (Ivezić et al. 2001)[4] of this object are reported. These data show large variations in colour. It is important to note that the $v - i$ colour is greater than the $v - z$ one,[5] which suggests the presence of an absorption band around 1 μm.

Visible spectroscopy of Frostia was reported by Alvarez-Candal et al. (2006). These results are in agreement with SDSS colours and the authors classified this asteroid in the V-taxonomic class.

The NIR spectrum of (854) Frostia (Fig. 1) was obtained on 2007 March 13. The total integration time of 40 min allows an accurate spectrum with S/N of 120. Following the Bus–DeMeo taxonomy, the NIR spectrum is typical of V-type asteroids (DeMeo et al. 2009).[6]

3.2 (1333) Cevenola

Dynamically, (1333) Cevenola belongs to the Eunomia family (Zappala et al. 1995; Mothé-Diniz, Roig & Carvano 2005). Photometry of this asteroid shows a large amplitude of 0.97 ± 0.03 mag and a synodical period of 4.88 ± 0.02 h (Warner 2002). The visible spectrum was reported by Lazzaro et al. (2004) in the framework of a S^{3}OS^2 survey, and the analysis of spectral data places the asteroid into the S (S_q more precisely) complex. The Eunomia family is actually dominated by objects displaying S-type spectra.

Two NIR spectra were obtained for this asteroid (Figs 2 and 3) on two consecutive nights, separated by 24 h. The spectrum of 2007 March 12 is the result of the combination of individual spectra of duration 120 s each for a total integration time of 1 h 28 min. The second spectrum was obtained on 2007 March 13 for a total integration time of 40 min. Consequently, S/N values of 50 and 20 was estimated.

The NIR spectra are very similar. The consistency with the S_q classification (DeMeo et al. 2009) is confirmed either based on NIR data or composite visible+NIR data.

3.3 (3623) Chaplin

(3623) Chaplin belongs to the Koronis family (Zappala et al. 1995; Mothé-Diniz et al. 2005). The asteroid has a synodic period of 8.361 ± 0.005 h and a large amplitude in its composite light curve,

[3] http://obswww.unige.ch/~behrend/page_cou.html
[4] http://sbn.psi.edu/ferret/
[5] The Sloan Digital Sky Survey was obtained using five broad-band filters, namely *u*, *g*, *r*, *i*, *z*, centred at 3551, 4686, 6165, 7481 and 8931 Å respectively.
[6] http://smass.mit.edu/busdemeoclass.html

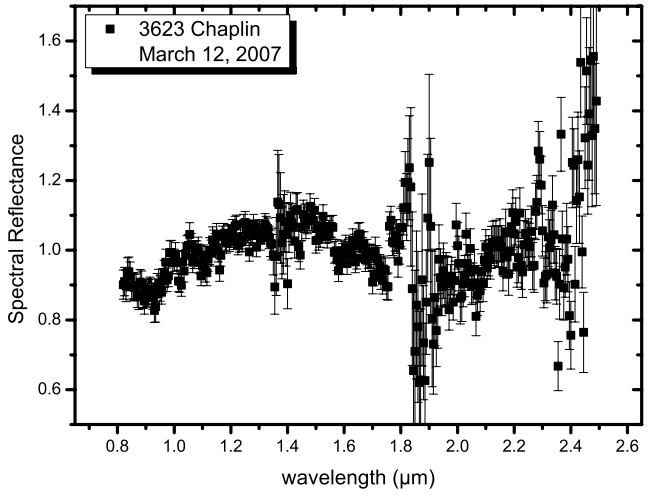

Figure 4. NIR spectrum of (3623) Chaplin obtained on 2007 March 12 with error bars. The spectrum is normalized to 1.25 μm.

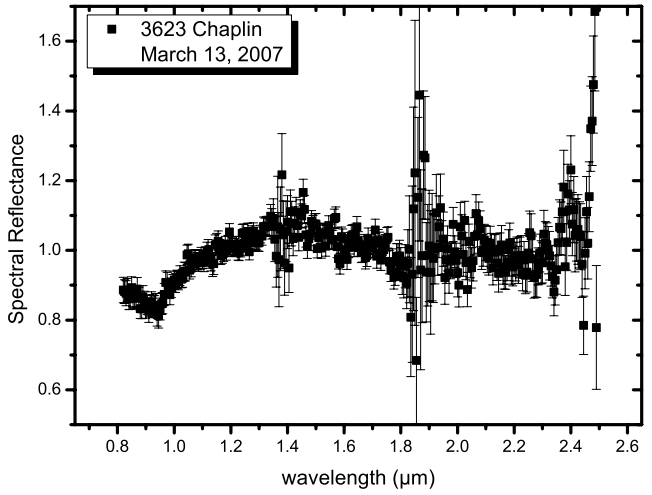

Figure 5. NIR spectrum of (3623) Chaplin obtained on 2007 March 13 with error bars. The spectrum is normalized to 1.25 μm.

estimated as 0.97 ± 0.02 mag (Birlan et al. 1996). There is no estimation for its pole coordinates.

Two NIR spectra of the asteroid, presented in Figs 4 and 5, were obtained at a time interval of about 23 h. The spectrum of 2007 March 12 is the result of combined individual spectra of duration 120 s each, for a total integration time of 72 min, while the the second spectrum (obtained on 2007 March 13) was obtained for a total integration time of 80 min. The S/N was estimated to be in the range 15–20.

The NIR spectrum is typical among S-complex asteroids (DeMeo et al. 2009), more precisely close to the S_q taxonomic subclass.

4 SPECTRAL MODELS AND MINERALOGICAL APPROACH

The three objects present absorption features around 1 and 2 μm, and the strength of absorption varies from one asteroid to another. The investigation was conducted using several techniques, namely the modified Gaussian model (Sunshine & Pieters 1993) and 2D mineralogical charts using χ^2 minimization of laboratory spectra.

4.1 Modified Gaussian model applied to spectra

The spectra were analysed using the modified Gaussian model (MGM) procedure (Sunshine & Pieters 1993). The procedure applied to high-quality spectral data allows the quantitative characterization of absorption features, by simultaneous fitting of multiple Gaussian-like absorption bands (Pieters & McFadden 1994). This condition is satisfied in our case for the spectra of Frostia and Cevenola, and in a relative way by the spectrum of Chaplin. The advantage of this method is the ability to compare the asteroid spectra quantitatively with certain minerals (Sunshine, Pieters & Pratt 1990) by calculating individual band centres, full width at half-maximum and strength. However, in the case of asteroid spectra, the results are physically relevant when the steps are carefully tested using laboratory measurements as standard (Canas, Duffard & Seixas 2008). This method is appropriate for spectra revealing absorption features. The method is unable to solve, in terms of a mineralogical solution, the continuum of analysed spectra.

The MGM approach was initially used in free parameter mode, by considering the best fit obtained with a minimum number of absorption bands, in an a priori assumption of mineralogical compounds. In a second step, depending on the minerals, the parameters of the continuum were fixed as well as the parameters of some individual absorption bands. We used the constraints obtained by Sunshine & Pieters (1998) for olivine while pyroxene was constrained by the results published by Cloutis & Gaffey (1991a). The MGM analysis was performed for Cevenola by taking advantage of previous work done by Sunshine et al. (2004) on S-type asteroids. The non-uniqueness of the mineralogical solution obtained from spectral modelling justifies the omission of minor components. The majority of the best mineralogical solutions from the literature (for the same sample) are reliable in a limit of a few per cent. Even at this level of confidence, the mineralogy is not unique. Thus, our approach is justified. Parameters of mineralogical solutions are presented in Table 3.

A mineralogical solution was obtained for (854) Frostia using five absorption bands (Fig. 6). This model shows that spectral features indicate the presence of both low-Ca pyroxene (LCP) and high-Ca pyroxene (HCP). The presence of HCP is required for the spectral fit at wavelengths larger than 2.1 μm. This band over 2.1 μm is a specific behaviour of type-B pyroxene, with bands attributable to crystal-field transitions in ferrous iron located in the M2 crystallographic site (Cloutis & Gaffey 1991b). For the spectral profile around 1.25 μm, the presence of plagioclase such as feldspar may be plausible. We note that the presence of absorption bands for olivine in the MGM analysis is not necessary for the fit of telescopic data.

The composite spectrum contained the visible data from the S^3OS^2 programme and our NIR data for (1333) Cevenola obtained on 2007 March 12 was also investigated using six absorption bands. In the model we used three absorption bands for the olivine in the 1-μm region (Sunshine & Pieters 1998). The band at 2.05 μm is recovered by only one pyroxene band with a good fit. Finally the fit was obtained by fixing the continuum and the width of absorption bands for the olivine. The model (Fig. 7) is relatively good within a limit of 1.6 per cent. Finally, the band at 1 μm is reproduced by four bands superimposed, implying the presence of both olivine and pyroxenes.

4.2 χ^2 best fit with RELAB data

The spectral properties of minerals in an intimate mixture combine in a non-additive, generally unique manner (Singer 1981). In the

Table 3. Modified Gaussian model applied to (854) Frostia and (1333) Cevenola. The best fit of this tool is summarized as follows: number of bands, centre of the band, full width at half-maximum value, absorption strength and slope of the continuum.

Asteroid	Number of bands	Centre of band (μm)	FWHM (μm)	Strength (log reflectance)	Continuum slope
		0.922	0.162	−0.359	
		1.032	0.202	−0.173	
(854) Frostia	5	1.248	0.150	−0.064	−5.10 E-05
		1.933	0.522	−0.414	
		2.330	0.546	−0.223	
		0.482	0.278	−0.196	
		0.851	0.239	−0.100	
(1333) Cevenola	6	0.916	0.184	−0.099	−7.12 E-06
		1.045	0.177	−0.118	
		1.220	0.459	−0.097	
		2.041	0.570	−0.130	

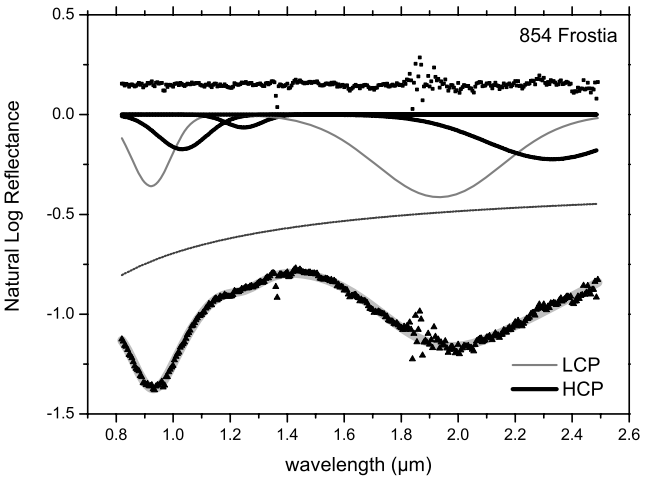

Figure 6. MGM modelling of NIR data of (854) Frostia using five absorption bands of low-Ca pyroxene (LCP) and high-Ca pyroxene (HCP). This figure presents, from bottom to top, the observational data superimposed on the MGM fit, the continuum, the individual absorption bands and the errors between the model and the observational data. These plots are offset for clarity.

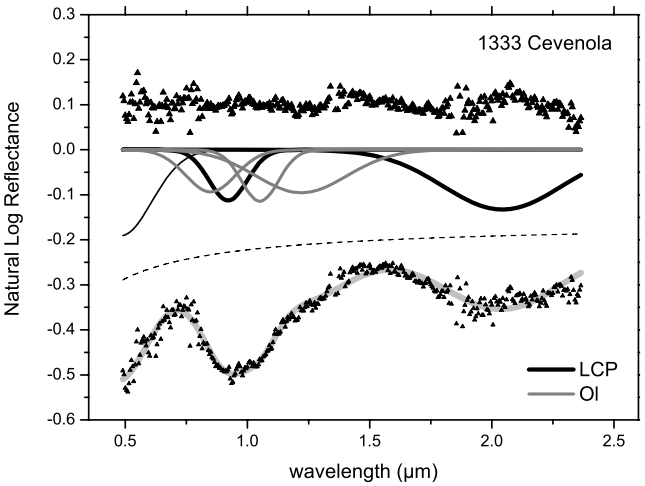

Figure 7. MGM modelling of VNIR data of (1333) Cevenola. The presence of both olivine (Ol) and pyroxene (LCP) minerals is necessary for this fit. The individual absorption bands are drawn in black for LCP and grey for olivine.

case of pyroxenes, this non-linearity was also presented by Cloutis & Gaffey (1991a). However, no other analytical law or approach by polynomial function was proposed until now for modelling real spectra. Thus, we propose the approach of three component minerals linearly mixed as a possible/probable solution to find families of minerals that are the best matches for our telescopic data.

The spectra were investigated with three-component mixtures. This is the first time that mineralogical χ^2 residual space has been plotted for asteroids. The initial components used for the mixtures are real laboratory spectra from the RELAB data base.[7]

In order to have a homogeneous data set, the end members were selected from the spectra obtained in the 0.3–2.6 μm wavelength range using the bidirectional visual and infrared spectrometer (BD-VNIR) within the Planetary Geology and Geophysics programme (PGG). The olivine (Ol), orthopyroxene (OPx) and clinopyroxene (CPx)[8] sets that were identified contain 44, 33 and 55 spectra respectively. The olivine set includes synthetic spectra that span the Fa_0Fo_{100}–$Fa_{100}Fo_0$ domain in 5–10 mol per cent increments (Dyar et al. 2009) while the members of orthopyroxene set sample the range En_0Fs_{100}–$En_{100}Fs_0$ (Klima, Pieters & Dyar 2007). The clinopyroxene spectra represents minerals with different Wo, En and Fs content. The wide variety of minerals included in the three above sets makes them suitable for generating spectra of synthetic mixtures.

The high-resolution, high-S/N RELAB spectra were fitted using a cubic B-spline function with 25 fitting coefficients. For the asteroid spectra, in order to avoid overfitting, the number of coefficients was reduced to 12. In both cases it was confirmed by visual inspection that the interpolating functions approximate well the overall shape of the spectra.

For each possible combination of olivine, ortho- and clinopyroxene, synthetic spectra were generated from *b*-splined end-member spectra using a linear mixture by varying the end-member concentration in 0.5 per cent increments (steps). Each of the obtained spectra was compared with spline smoothed spectra of (854) Frostia, (1333) Cevenola and (3623) Chaplin. The χ^2 calculations

[7] http://www.planetary.brown.edu/relab
[8] Structures of orthorhombic and monoclinic crystals of pyroxenes.

were performed following the formula

$$\chi^2 = \frac{1}{N_w} \sum_{i=1}^{N_w} \frac{[R_i - f(w_i)]^2}{f(w_i)}, \quad (1)$$

where N_w is the number of R_i reflectance values at wavelength w_i and $f(w_i)$ is the reflectance value of the geometric mixture obtained from laboratory spectra (i.e. additive contribution of individual components).

The concentration for each of the components will span the range 0–100 per cent and the sum of the mixture is 100 per cent. The best mixture identified by the above χ^2 test is further refined in 0.1 per cent concentration steps this time with fixed end members.

The χ^2 minimization will allow the derivation of a map of possible/plausible models. This method allows the plot of 2D mineralogical charts, an interesting tool for visualizing the best mineralogical solutions.

Two-dimensional charts derived from the χ^2 fit are presented in Figs 8, 9 and 10 for (854) Frostia, (1333) Cenevola and (3623) Chaplin respectively. These charts plot olivine on the X axis and OPx/(CPx+OPx) on the Y axis. The colour code indicates the concordance of the model with the observational data, the blue colour representing the best fit. The white regions of the 2D charts are an indicator of the limit where the χ^2 minimization fails.

The best-fitting mixture for (854) Frostia was obtained using (Ol, OPx, CPx) = (0, c1dl14, c1dl07) with ratios of (0 per cent, 33.5 per cent, 66.5 per cent). For the asteroid (1333) Cevenola, the best fit was obtained using (Ol, OPx, CPx) = (cgpo84, c1dl01, c1dl12) with ratios of (25 per cent, 67.5 per cent, 7.5 per cent).

In the case of (3623) Chaplin, the closest analogue was the mixture (0, c1dl01, c1dl08) with ratios of (0 per cent, 96.5 per cent, 3.5 per cent).

The inferred mineralogical solutions explain the asteroid spectra well. However, given the inherent complications of a curve-matching procedure such as the χ^2 test (Gaffey et al. 2002), a family of mineralogical solutions could fit our spectroscopic data.

5 DISCUSSION

The binarity of (854) Frostia is supported by photometric data (Behrend et al. 2006). Unfortunately, no physical ephemerides of Frostia are known to have a precise timing of possible mutual phenomena of this system. Nevertheless, there is little chance of a geometry allowing mutual phenomena at the time of our observations. The spectrum likely represents this object globally, thus being a first attempt at the characterization of the asteroid's mineralogy.

The spectrum of (854) Frostia (Fig. 1) reveals large and deep absorption bands around 1 and 2 μm. This spectrum, similar to that

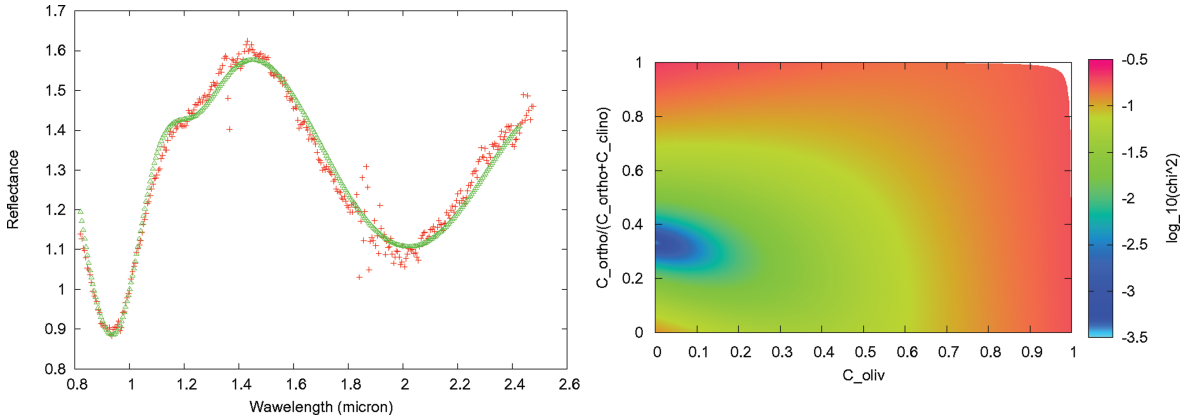

Figure 8. A two-dimensional chart of concentration for the asteroid (854) Frostia using olivine, orthopyroxene and clinopyroxene from RELAB is presented on the right side of the figure. The best-fitting mixture for (854) Frostia using (Ol, OPx, CPx) = (0, c1dl14, c1dl07) with ratios (0 per cent, 33.5 per cent, 66.5 per cent) is presented on the left side of the figure.

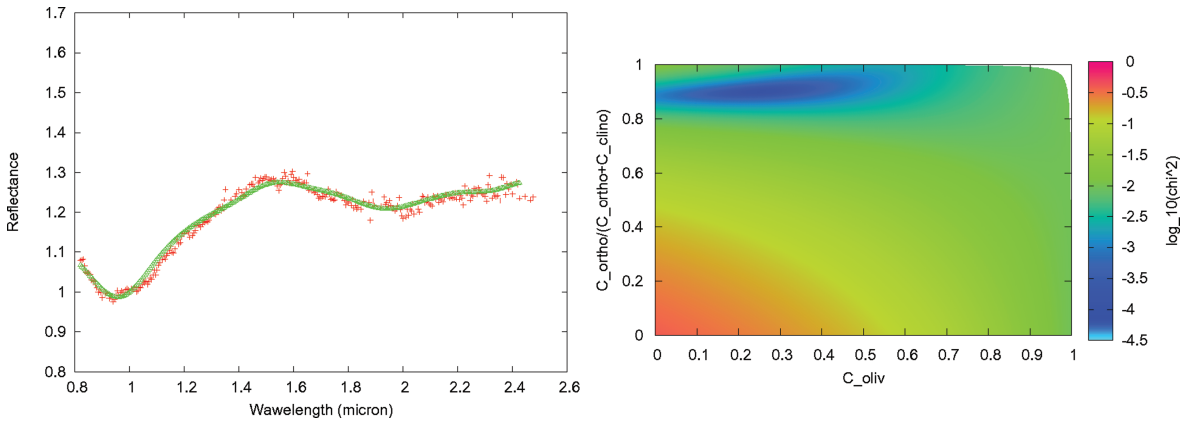

Figure 9. A two-dimensional chart of concentration for the asteroid (1333) Cevenola using olivine, orthopyroxene and clinopyroxene from RELAB is presented on the right side of the figure. The best mineralogical model for (1333) Cevenola using (Ol, OPx, CPx) = (cgpo84, c1dl01, c1dl12) and the ratios (25 per cent, 67.5 per cent, 7.5 per cent) is presented on the left side of the figure.

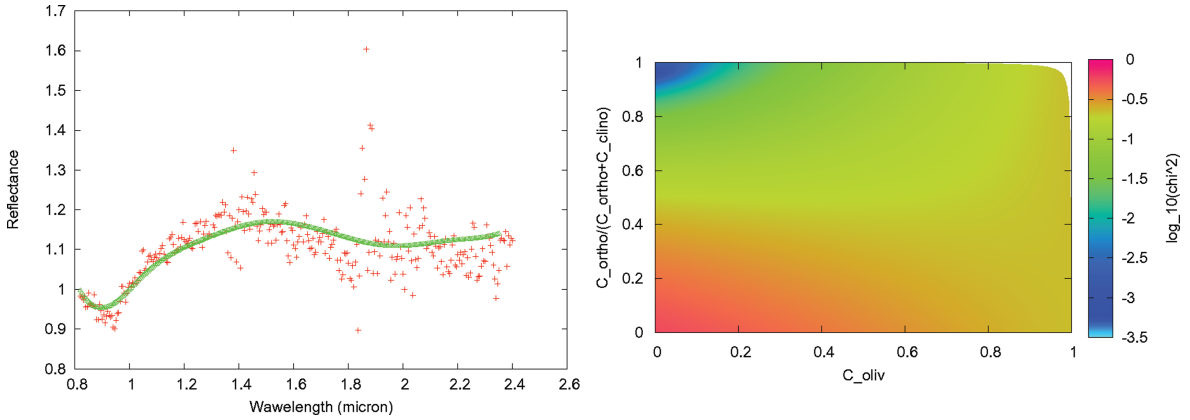

Figure 10. A two-dimensional chart of concentration for the asteroid (3623) Chaplin using olivine, orthopyroxene and clinopyroxene from RELAB. The best mineralogical mixture using (Ol, OPx, CPx) = (0, c1dl01, c1dl08) with ratios (0 per cent, 96.5 per cent, 3.5 per cent) is presented on the left side of the figure.

of asteroid (4) Vesta, allows the classification of (854) Frostia in the V-type taxonomic class. Based on spectroscopic behaviour and dynamical consideration from the main belt through the 3:1 and ν_6 resonances (Binzel & Xu 1993), Vesta and the vestoids are supposed to be the origin of Howardite–Eucrite–Diogenite (HED) meteorites. The structure of HED meteorites is very close to that of mafic materials. Thus, the parent body of HED meteorites is supposed to have experienced volcanism and metamorphism in the process of formation during the early solar system. The parent body of Vesta and vestoids underwent accretion, total melting, fractionation and differentiation during the first few million years of solar-system formation (Keil 2002).

(854) Frostia was not included in the family of (4) Vesta by Zappala et al. (1995). The location of (854) Frostia inside the main belt is very similar to that of the Vesta family in semimajor axis and inclination and may justify its membership of the same clan. Frostia's eccentricity of 0.17 is slightly over the greater boundary (0.12) of the Vesta family. This case is not unique, while other V-type asteroids were already reported in the inner part of the main belt, relatively close to the Vesta family (Duffard et al. 2004).

The V-type asteroids are objects with reflectance spectra similar to those of asteroid (4) Vesta and HED meteorites. Vesta is considered as *the smallest terrestrial planet* (Keil 2002) and is a differentiated object with a basaltic crust and exposed mantle material (Gaffey 1997) that survived almost intact during the solar-system history. Objects smaller in size than Vesta (commonly called 'vestoids') present spectral properties similar to this asteroid. Partly the vestoids are identified as fragments of Vesta, a result of a catastrophic collision that excavated material from the crust and mantle (Binzel & Xu 1993) of Vesta. Vesta's density was derived from the estimation of its mass (Hilton 2002) and shape (Thomas et al. 1997). The computed values of the bulk density span the range 3000–4300 kg m^{-3} (Birlan 2000). This interval is supported also by models of internal structure of large differentiated bodies. Ruzicka, Snyder & Taylor (1997) calculated the density of the silicate fraction in Vesta-like asteroids, assuming an average value of the bulk density of 3540 kg m^{-3}. They conclude that Vesta could be modelled with an eucritic/diogenitic crust and olivine mantle for a metallic core between zero and 25 per cent of the total mass of the asteroid. In this case, the density of the crust could not be less than 3000 kg m^{-3}.

In the assumption of (854) Frostia as a fragment of Vesta's crust, a value of its density around 3000 kg m^{-3} seems to be reasonable. The value calculated by Behrend et al. (2006) (around 1000 kg m^{-3}) is very difficult to explain even if we assume unrealistic porosities of 75 per cent in a rubble-pile structure. In fact, large porosities for small fragments of large differentiated bodies are not realistic, while the self-gravitation tendency is to decrease the volume of empty space inside the object. Behrend et al. (2006) inferred a C-type asteroid by analogy with the asteroid (90) Antiope. It is difficult to reconcile the C and V taxonomic classes, while the objects experienced different temperatures in their history.

Descamps (2010) recently published a refined study of binary systems by accounting for inhomogeneous bodies with ellipsoidal shapes. This model allows the simultaneous fit of grain density and bulk porosity. The author calculated a grain density of (2, 790 ± 380) kg m^{-3}, in agreement with that of Vesta-like asteroids, correlated to a bulk porosity of 63 per cent (≈55 per cent macroscopic porosity + ≈8 per cent microporosity).

The mineralogy of (854) Frostia could be refined by taking into account the precise position of the band centres at 1 and 2 μm. To estimate the minima of these absorption features, we removed the continuum by considering a linear function for each one. The continuum for Band I was estimated using the reflectances at 0.7 and 1.43 μm, while for Band II the continuum was estimated using the reflectances at 1.43 and 2.49 μm respectively. While our spectrum does not contains the reflectance at 0.7 μm, this value was estimated by polynomial extrapolation. The reflectance at 0.7 μm usually represents the lower limit of the 1-μm absorption feature for V-type asteroids (Duffard et al. 2004; Vernazza et al. 2005). The continuum was then extracted from the spectrum in each corresponding region. The band centre was then computed using a sixth-order polynomial function. We found that the Band I minimum is located at 0.931 ± 0.004 μm, while the Band II minimum is located at 1.976 ± 0.004 μm. In the case of Band I, we calculated the thermal correction using formulae (2) and (4) from Burbine et al. (2009). This value is 0.002 μm, within the value of the error bar for the Band I centre; thus we can neglect its influence. The positions of Band I and Band II centres are relatively similar to those obtained for the asteroid (1459) Magnya (Hardersen, Gaffey & Abell 2004). If we place these values for Frostia in the context of the pyroxene studies of Adams (1974) and Cloutis & Gaffey (1991a), we conclude a dominant presence of orthopyroxene on the asteroid surfaces. The position of the bands places the asteroid between the Eucrite and Diogenite regions (see fig. 6 of Hardersen et al. 2004). These results are partially confirmed by our Fig. 8, which presents a large dominance of orthopyroxene.

The spectrum of (854) Frostia presents an inflexion near 1.2 μm, which is an indication of the presence of feldspar in the basaltic achondrite materials. The mineralogical composition using the pyroxene calibration (Gaffey et al. 2002) suggests the formula $Wo_8Fs_{43}En_{49}$ (with a 4 per cent of uncertainty for wollastonite and ferrosilite). This composition is, within the error bars, similar to that of (4) Vesta and (1459) Magnya, and similar to that of the asteroid (3269) De Sanctis (Duffard et al. 2004).

Another important mineralogical parameter that was investigated for (854) Frostia was the band-area ratio (BAR). This is the result of the ratio between Bands I and II. The Band I area was calculated as the area between the continuum defined by the correspondent reflectances at 0.7 and 1.4 μm and the spectrum. The Band II area was calculated as the area between the continuum defined by the correspondent reflectances at 1.4 and 2.43 μm and the spectrum. The reflectance value at 0.7 μm was estimated by linear extrapolation. Depending on the range that this value could span, the estimation for the area of Band I could differ by up to 5 per cent. This extrapolation of our spectrum is also in agreement with the visible spectrum of Alvarez-Candal et al. (2006). The procedure of computation for the BAR value was prior tested and validated using two spectra of V-type asteroids (4) Vesta and (1459) Magnya (R. Binzel, personal communication). The calculated BAR for (854) Frostia was 1.57±0.08, in agreement with the basaltic achondrite minerals (Gaffey et al. 1993).

V-type asteroids are mainly located in the population represented by the Vesta family, and are considered to be the reservoir of HED meteorites. However, basaltic asteroids, not yet considered members of the Vesta family, are also located in the vicinity of the family (Florczak, Lazzaro & Duffard 2002; Duffard et al. 2004). Data on V-type asteroids such as (1459) Magnya are reported at different semimajor axes (Lazzaro et al. 2000; Roig & Gil-Hutton 2006; Duffard & Roig 2009) and in the near-Earth asteroid population (Binzel et al. 2002). This picture of V-type asteroids supports the hypothesis of the formation of several objects with basaltic crust in the main belt. The plot of Band I centre versus BAR exhibits a diversity among V-type asteroids much larger than the one obtained for basaltic achondrite meteorites. This extension of the BAR range may be explained by reconsidering the physics and mineralogy of asteroid surfaces.

The asteroid (1333) Cevenola is a member of the Eunomia family, which numbers more than 430 objects (Zappala et al. 1995). 44 members of this family (including Cevenola) were studied spectroscopically in the visible region by Lazzaro et al. (1999). 41 of them were classified as S-type objects, while three asteroids exhibit flat spectra and were considered as interlopers. If we consider this sample in the frame of the Bus–DeMeo taxonomy (DeMeo et al. 2009), only three objects are re-observed in the near-infrared region. A robust conclusion about this family cannot be drawn in the Bus–DeMeo taxonomic system, however we can speculate on a S_q taxonomic type for the three objects considering the VNIR data.

The MGM analysis (Fig. 7) strongly indicates that the presence of both olivine and pyroxene is necessary for reproducing the observational data of (1333) Cevenola. The mineralogical solution corresponds to fayalitic material with molar percentage equal to 20 ± 5 (Sunshine et al. 2007) and the width of these absorption bands spans the same range in presented in Sunshine & Pieters (1998). However, the strength ratio between the M1 and M2 olivine crystals is different from the calibration values proposed by Sunshine et al. (2007). This implies that mineralogies with fayalitic–forsteritic components need to be completed with other components. Recently, Isaacson & Pieters (2010) proposed a mineralogical solution of surfaces of Mars rich in olivine, by considering the spectral influence of chromites. The effect of chromite in olivine minerals is observed in the reduced reflectance and in the absorption feature beyond 1.5 μm. A similar mineralogical solution, together with solutions obtained from different olivine varieties (dunite, peridot, chryolithe, wadsleyite), needs future analysis.

The family of mineralogical solutions computed by the χ^2 composition map (Fig. 9) for (1333) Cevenola is also composed of a mixture of ortopyroxene and olivine (the horizontal dark-blue region in the figure). The olivine is less constrained, ranging from 0–60 per cent. This region is completed by the blue part of the map for high olivine percentages. In this case, the family of mineralogical solutions is less constrained than that obtained for (854) Frostia.

Following DeMeo et al. (2009) the S_q asteroids 'present a wide 1 μm absorption band with evidence of a feature near 1.3 μm like the Q-type, except the 1 μm feature is more shallow' for this class. (1333) Cevenola is similar to the S–IV mineralogical subtype (Gaffey et al. 1993). Following Gaffey et al. (1993), this subclass is characterized by assemblages of olivine–orthopyroxene, which could represent assemblages similar to either undifferentiated ordinary chondrites or the unmelted silicate portions of primitive achondrites.

(3623) Chaplin is a member of the Koronis family. The NIR spectrum spans the same characteristics as the S-type complex, which is the taxonomic class of the Koronis family. We extrapolate its thermal albedo to that of the S-class of 0.198 ± 0.067 (Fulchignoni, Birlan & Antonietta Barucci 2000). The mineralogical map obtained in section 4.2 (dark region in the mineralogical map) shows a best fit for families of mineralogical solutions dominated by orthopyroxene with clinopyroxenes and olivine as minor constituents.

(1333) Cevenola and (3623) Chaplin were observed over two consecutive nights in order to detect variations in their spectra. Their correspondent spectra have the same profile, which is interpreted as a homogeneity of the surfaces of each object.

6 CONCLUSIONS

0.8–2.5 μm spectral data were obtained and analysed for the main-belt asteroids (854) Frostia, (1333) Cevenola and (3623) Chaplin. This NIR spectral interval is covered for the first time for our targets, chosen from among those asteroids with large amplitudes in their light curves that were observed previously photometrically. Detailed mineralogical analysis using a modified Gaussian model was performed for our objects. New techniques such as 2D spectral charts by a χ^2 fit of mineralogical assemblages were performed for (854) Frostia and (1333) Cevenola.

The asteroid (854) Frostia was classified as V-type, for which the density and the spectral properties are incompatible with the previous findings on density. The spectral properties of this object are similar to those of basalts. We calculated the mineralogical solution $Wo_8Fs_{43}En_{49}$, with an error of 4 per cent in wollastonite and ferrosilite, for Frostia.

(1333) Cevenola is a member of the Eunomia family and belongs to the S_q taxonomic type. Mineralogical maps were constructed for the first time for (854) Frostia and (1333) Cevenola, using as end members the available laboratory data for olivine, ortho- and clinopyroxenes.

Finally, (3623) Chaplin belongs to the S-type taxonomic complex, which characterizes members of the Koronis family. Its mineralogy corresponds to minerals with olivine and pyroxene content.

ACKNOWLEDGMENTS

This article is based on observations acquired with InfraRed Telescope Facilities as well as the CODAM remote facilities. We thank all the telescope operators for their contribution. This research utilizes spectra acquired with the NASA RELAB facility at Brown University. The authors thank Francesca DeMeo and Rick Binzel for careful reading and pertinent remarks. The work of DAN was partially supported by the Romanian National Authority for Scientific Research (ANCS) under the project POSCCE-A2-O2.1.2-2009-2/651. We thank the anonymous referee for useful remarks. This article uses observations performed with SpeX/IRTF.

REFERENCES

Adams J. B., 1974, J. Geophys. Res., 79, 4829
Alvarez-Candal A., Duffard R., Lazzaro D., Michtchenko T., 2006, A&A, 459, 969
Behrend R. et al., 2006, A&A, 446, 1177
Binzel R. P., 1978, Minor Planet Bulletin, 6, 18
Binzel R. P., van Flandern T. C., 1979, Sci, 203, 903
Binzel R. P., Xu S., 1993, Sci, 260, 186
Binzel R. P., Lupishko D., di Martino M., Whiteley R. J., Hahn G. J., 2002, in Bottke W. F., Jr, Cellino A., Paolicchi P., Binzel R. P., eds, Asteroids III. Univ. Arizona Press, Tucson, p. 255
Birlan M., 2000, Earth Moon and Planets, 88, 1
Birlan M., Barucci M. A., Angeli C. A., Doressoundiram A., de Sanctis M. C., 1996, Planet. Space Sci., 44, 555
Birlan M., Barucci M. A., Vernazza P., Fulchignoni M., Binzel R. P., Bus S. J., Belskaya I., Fornasier S., 2004, New Astron., 9, 343
Birlan M., Vernazza P., Fulchignoni M., Barucci M. A., Descamps P., Binzel R. P., Bus S. J., 2006, A&A, 454, 677
Burbine T. H., Buchanan P. C., Dolkar T., Binzel R. P., 2009, Meteoritics and Planetary Science, 44, 1331
Canas L., Duffard R., Seixas T., 2008, Earth Moon and Planets, 102, 543
Cellino A., Pannunzio R., Zappala V., Farinella P., Paolicchi P., 1985, A&A, 144, 355
Cloutis E. A., Gaffey M. J., 1991a, J. Geophys. Res., 96, 22809
Cloutis E. A., Gaffey M. J., 1991b, Earth Moon and Planets, 53, 11
Cushing M. C., Vacca W. D., Rayner J. T., 2004, Planet. Space Sci., 116, 362
Dell'Oro A., Cellino A., 2007, MNRAS, 380, 399
DeMeo F. E., Binzel R. P., Slivan S. M., Bus S. J., 2009, Icarus, 202, 160
Descamps P., 2010, Icarus, 207, 758
Descamps P., Marchis F., Michalowski T., Vachier F., Colas F., Berthier J., Assafin M., Dunckel P. B. A., 2007, Icarus, 187, 482
Donnison J. R., 1979, MNRAS, 186, 35P
Duffard R., Roig F., 2009, Planet. Space Sci., 57, 229
Duffard R., Lazzaro D., Licandro J., de Sanctis M. C., Capria M. T., Carvano J. M., 2004, Icarus, 171, 120
Dunlap J. L., Gehrels T., 1969, AJ, 74, 796
Durda D. D., Bottke W. F., Enke B. L., Merline W. J., Asphaug E., Richardson D. C., Leinhardt Z. M., 2004, Icarus, 170, 243
Dyar M. et al., 2009, American Mineralogist, 94, 883
Florczak M., Lazzaro D., Duffard R., 2002, Icarus, 159, 178
French L. M., Binzel R. P., 1989, in Binzel R. P., Gehrels T., Matthews M. S., eds, Asteroids II. Univ. Arizona Press, Tucson, p. 54
Fulchignoni M., Birlan M., Antonietta Barucci M., 2000, Icarus, 146, 204
Gaffey M. J., 1997, Icarus, 127, 130
Gaffey M. J., Burbine T. H., Piatek J. L., Reed K. L., Chaky D. A., Bell J. F., Brown R. H., 1993, Icarus, 106, 573
Gaffey M. J., Cloutis E. A., Kelley M. S., Reed K. L., 2002, in Bottke W. F., Jr, Cellino A., Paolicchi P., Binzel R. P., eds, Asteroids III. Univ. Arizona Press, Tucson, p. 183
Hardersen P. S., Gaffey M. J., Abell P. A., 2004, Icarus, 167, 170
Harris A. W., Lupishko D. F., 1989, in Binzel R. P., Gehrels T., Matthews M. S., eds, Asteroids II. Univ. Arizona Press, Tucson, p. 39
Hilton J. L., 2002, in Bottke W. F., Jr, Cellino A., Paolicchi P., Binzel R. P., eds, Asteroids III. Univ. Arizona Press, Tucson, p. 103
Holsapple K. A., Michel P., 2008, Icarus, 193, 283
Isaacson P. J., Pieters C. M., 2010, Icarus, 210, 8
Ivezić Ž. et al., 2001, AJ, 122, 2749
Keil K., 2002, in Bottke W. F., Jr, Cellino A., Paolicchi P., Binzel R. P., eds, Asteroids III. Univ. Arizona Press, Tucson, p. 573
Klima R. L., Pieters C. M., Dyar M. D., 2007, Meteoritics and Planetary Science, 42, 235
Lagerkvist C., Barucci M. A., Capria M. T., Fulchignoni M., Guerriero L., Perozzi E., Zappala V., 1987, Asteroid photometric catalogue
Lazzaro D. et al., 1999, Icarus, 142, 445
Lazzaro D. et al., 2000, Sci, 288, 2033
Lazzaro D., Angeli C. A., Carvano J. M., Mothé-Diniz T., Duffard R., Florczak M., 2004, Icarus, 172, 179
Leone G., Paolicchi P., Farinella P., Zappala V., 1984, A&A, 140, 265
Magri C., Nolan M. C., Ostro S. J., Giorgini J. D., 2007, Icarus, 186, 126
Marchis F., Descamps P., Hestroffer D., Berthier J., 2005, Nat, 436, 822
Mothé-Diniz T., Roig F., Carvano J. M., 2005, Icarus, 174, 54
Ostro S. J. et al., 2000, Sci, 288, 836
Ostro S. J., Hudson R. S., Benner L. A. M., Giorgini J. D., Magri C., Margot J. L., Nolan M. C., 2002, in Bottke W. F., Jr, Cellino A., Paolicchi P., Binzel R. P., eds, Asteroids III. Univ. Arizona Press, Tucson, p. 151
Pieters C. M., McFadden L. A., 1994, Ann. Rev. Earth and Planetary Sci., 22, 457
Pravec P., Šarounová L., Hicks M. D., Rabinowitz D. L., Wolf M., Scheirich P., Krugly Y. N., 2002, Icarus, 158, 276
Rayner J. T., Toomey D. W., Onaka P. M., Denault A. J., Stahlberger W. E., Vacca W. D., Cushing M. C., Wang S., 2003, PASP, 115, 362
Rivkin A. S., Binzel R. P., Sunshine J., Bus S. J., Burbine T. H., Saxena A., 2004, Icarus, 172, 408
Roig F., Gil-Hutton R., 2006, Icarus, 183, 411
Ruzicka A., Snyder G. A., Taylor L. A., 1997, Meteoritics and Planetary Science, 32, 825
Singer R. B., 1981, J. Geophys. Res., 86, 7967
Storrs A., Weiss B., Zellner B., Burleson W., Sichitiu R., Wells E., Kowal C., Tholen D., 1999, Icarus, 137, 260
Sunshine J. M., Pieters C. M., 1993, J. Geophys. Res., 98, 9075
Sunshine J. M., Pieters C. M., 1998, J. Geophys. Res., 103, 13675
Sunshine J. M., Pieters C. M., Pratt S. F., 1990, J. Geophys. Res., 95, 6955
Sunshine J. M., Bus S. J., McCoy T. J., Burbine T. H., Corrigan C. M., Binzel R. P., 2004, Meteoritics and Planetary Science, 39, 1343
Sunshine J. M., Bus S. J., Corrigan C. M., McCoy T. J., Burbine T. H., 2007, Meteoritics and Planetary Science, 42, 155
Tedesco E. F., 1979, Sci, 203, 905
Thomas P. C., Binzel R. P., Gaffey M. J., Zellner B. H., Storrs A. D., Wells E., 1997, Icarus, 128, 88
Vacca W. D., Cushing M. C., Rayner J. T., 2004, PASP, 116, 352
van Flandern T. C., Tedesco E. F., Binzel R. P., 1979, in Gehrels T., ed., Satellites of asteroids. Asteroids. Univ. Arizona Press, Tucson, p. 443
Vernazza P., Mothé-Diniz T., Barucci M. A., Birlan M., Carvano J. M., Strazzulla G., Fulchignoni M., Migliorini A., 2005, A&A, 436, 1113
Warner B. D., 2002, Minor Planet Bull., 29, 74
Wijesinghe M. P., Tedesco E. F., 1979, Icarus, 40, 383
Zappala V., Scaltriti F., Farinella P., Paolicchi P., 1980, Moon and Planets, 22, 153
Zappala V., Bendjoya P., Cellino A., Farinella P., Froeschle C., 1995, Icarus, 116, 291

This paper has been typeset from a TEX/LATEX file prepared by the author.